Hepatic FcRn regulates albumin homeostasis and susceptibility to liver injury

Michal Pyzik[a,1], Timo Rath[a,1,2], Timothy T. Kuo[a,1], Sanda Win[b], Kristi Baker[a,3], Jonathan J. Hubbard[a,c,d], Rosa Grenha[a], Amit Gandhi[a], Thomas D. Krämer[a,4], Adam R. Mezo[e,5], Zachary S. Taylor[e,6], Kevin McDonnell[e], Vicki Nienaber[f], Jan Terje Andersen[g,h], Atsushi Mizoguchi[i,j,k,7], Laurence Blumberg[l], Shalaka Purohit[l], Susan D. Jones[l], Greg Christianson[m], Wayne I. Lencer[c,d], Inger Sandlie[g,h], Neil Kaplowitz[b], Derry C. Roopenian[m], and Richard S. Blumberg[a,8]

[a]Department of Medicine, Division of Gastroenterology, Hepatology and Endoscopy, Brigham and Women's Hospital, Harvard Medical School, Boston, MA 02115; [b]Research Center for Liver Diseases, Keck School of Medicine, University of Southern California, Los Angeles, CA 90033; [c]Division of Gastroenterology and Nutrition, Children's Hospital Boston, Boston, MA 02115; [d]Department of Pediatrics, Harvard Medical School, Boston, MA 02115; [e]Biogen Idec-Hemophilia, Inc., Waltham, MA 02451; [f]Zenobia Therapeutics, Inc., San Diego, CA 92121; [g]Department of Immunology, Oslo University Hospital Rikshospitalet, University of Oslo, Oslo 0424, Norway; [h]Department of Biosciences, University of Oslo, Oslo 0316, Norway; [i]Center for the Study of Inflammatory Bowel Disease, Massachusetts General Hospital, Boston, MA 02114; [j]Molecular Pathology Unit, Massachusetts General Hospital, Charlestown 02129 MA; [k]Department of Pathology, Harvard Medical School, Boston 02115 MA; [l]Syntimmune Inc., New York, NY 10010; and [m]The Jackson Laboratory, Bar Harbor, ME 04609

Edited by Lawrence Steinman, Stanford University School of Medicine, Stanford, CA, and approved February 23, 2017 (received for review November 3, 2016)

The neonatal crystallizable fragment receptor (FcRn) is responsible for maintaining the long half-life and high levels of the two most abundant circulating proteins, albumin and IgG. In the latter case, the protective mechanism derives from FcRn binding to IgG in the weakly acidic environment contained within endosomes of hematopoietic and parenchymal cells, whereupon IgG is diverted from degradation in lysosomes and is recycled. The cellular location and mechanism by which FcRn protects albumin are partially understood. Here we demonstrate that mice with global or liver-specific FcRn deletion exhibit hypoalbuminemia, albumin loss into the bile, and increased albumin levels in the hepatocyte. In vitro models with polarized cells illustrate that FcRn mediates basal recycling and bidirectional transcytosis of albumin and uniquely determines the physiologic release of newly synthesized albumin into the basal milieu. These properties allow hepatic FcRn to mediate albumin delivery and maintenance in the circulation, but they also enhance sensitivity to the albumin-bound hepatotoxin, acetaminophen (APAP). As such, global or liver-specific deletion of FcRn results in resistance to APAP-induced liver injury through increased albumin loss into the bile and increased intracellular albumin scavenging of reactive oxygen species. Further, protection from injury is achieved by pharmacologic blockade of FcRn–albumin interactions with monoclonal antibodies or peptide mimetics, which cause hypoalbuminemia, biliary loss of albumin, and increased intracellular accumulation of albumin in the hepatocyte. Together, these studies demonstrate that the main function of hepatic FcRn is to direct albumin into the circulation, thereby also increasing hepatocyte sensitivity to toxicity.

FcRn | albumin | liver | bile | toxin

Albumin and IgG are the most long-lived and abundant circulating serum proteins. Their persistence is regulated by the neonatal crystallizable fragment receptor (FcRn), which binds both proteins in a pH-dependent manner, favoring interactions within intracellular organelles such as the endosome (1–3). In the case of monomeric IgG, binding to FcRn in acidic endosomes of endothelial and hematopoietic cells serves to recycle IgG to the cell surface where it is released into the circulation at physiologic pH (4, 5). In a similar manner, FcRn also mediates the bidirectional transport of IgG across a variety of polarized epithelial cells (6–9). This knowledge has led to therapeutic innovations that aim either to recombine biologic agents with the Fc fragment of IgG to enable FcRn interactions, thus prolonging the half-life of the therapeutic, or conversely to reduce the therapeutic agent's half-life by disabling binding to FcRn (10).

Less is known about the physiologic mechanisms that underlie albumin homeostasis through interactions with FcRn and what cell types are involved. Although albumin and IgG display pH-dependent binding to FcRn, the interaction surface, affinity, and mode of interaction differ between the two proteins (11–13). Still,

Significance

Neonatal crystallizable fragment receptor (FcRn) regulates immunity and homeostasis of the two most abundant circulating proteins, IgG and albumin. FcRn is expressed in hepatocytes, but hepatic FcRn function is unknown. We show that hepatic FcRn regulates albumin biodistribution. Absence of FcRn in the liver leads to hypoalbuminemia by preventing efficient albumin delivery into the circulation, causing albumin retention within hepatocytes and increasing biliary albumin excretion. Blockade of albumin–FcRn interactions protects liver from damage induced by acetaminophen, a hepatotoxin. This protection results from hepatocyte accumulation of albumin, which scavenges superoxide radicals, and from the redirection of albumin-bound acetaminophen into the bile. Therefore, FcRn-mediated homeostatic distribution of albumin into the bloodstream renders hepatocytes susceptible to acute hepatotoxin exposure, and inhibition of FcRn in the hepatocyte is protective.

Author contributions: M.P., T.R., T.T.K., S.W., K.B., R.G., A.R.M., J.T.A., L.B., S.P., W.I.L., I.S., N.K., D.C.R., and R.S.B. designed research; M.P., T.R., T.T.K., S.W., K.B., J.J.H., R.G., T.D.K., A.R.M., Z.S.T., K.M., V.N., J.T.A., A.M., S.D.J., and G.C. performed research; M.P., T.R., T.T.K., S.W., K.B., R.G., A.G., A.R.M., Z.S.T., K.M., V.N., J.T.A., and G.C. analyzed data; and M.P., T.R., and R.S.B. wrote the paper.

Conflict of interest statement: R.S.B., W.I.L., D.C.R., and I.S. serve as consultants to Syntimmune, Inc., which is developing therapeutic agents directed at FcRn.

This article is a PNAS Direct Submission.

Freely available online through the PNAS open access option.

Data deposition: Crystallography, atomic coordinates, and structure factors reported in this paper have been deposited in the Protein Data Bank (PDB ID code 5BJT).

[1]M.P., T.R., and T.T.K. contributed equally to this work.

[2]Present address: Department of Medicine, Division of Gastroenterology, Erlangen University Hospital, Friedrich Alexander University Erlangen-Nuremberg, 91054 Erlangen, Germany.

[3]Present address: Department of Oncology, Faculty of Medicine and Dentistry, University of Alberta, Edmonton, AB T6G 1Z2, Canada.

[4]Present address: Department of Nephrology and Hypertension Diseases, Hannover Medical School, 30169 Hannover, Germany.

[5]Present address: Lilly Research Laboratories, Eli Lilly and Company Lilly Corporate Center, Indianapolis, IN 46225.

[6]Present address: Department of Biological Sciences, Thomas More College, Crestview Hills, KY 41017.

[7]Present address: Department of Immunology, Kurume University School of Medicine, Kurume, 830-0011 Fukuoka, Japan.

[8]To whom correspondence should be addressed. Email: rblumberg@bwh.harvard.edu.

This article contains supporting information online at www.pnas.org/lookup/suppl/doi:10.1073/pnas.1618291114/-/DCSupplemental.

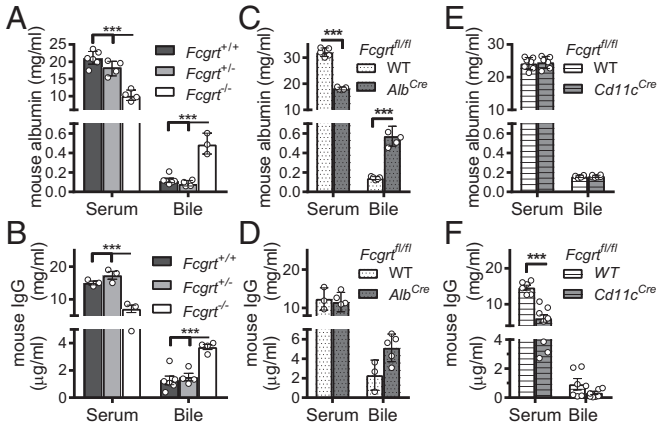

Fig. 1. FcRn deficiency causes albumin-losing biliopathy. (*A* and *B*) Bile and serum levels of mouse albumin (*A*) or IgG (*B*) in $Fcgrt^{-/-}$, $Fcgrt^{+/-}$, and $Fcgrt^{+/+}$ mice (n = 3–6 mice per group; ***$P < 0.001$). (*C* and *D*) Bile and serum levels of mouse albumin (*C*) or IgG (*D*) in WT ($Fcgrt^{fl/fl}$-*WT*) and *Fcgrt* liver-specific–deficient ($Fcgrt^{fl/fl}$-Alb^{Cre}) mice (n = 3–5; ***$P < 0.001$). (*E* and *F*) Bile and serum levels of mouse albumin (*E*) or IgG (*F*) in WT ($Fcgrt^{fl/fl}$-*WT*) mice and mice with CD11c-specific deletion of *Fcgrt* ($Fcgrt^{fl/fl}$-$Cd11c^{Cre}$) (n = 6–7; ***$P < 0.001$). Data were statistically analyzed by two-way ANOVA with Fisher's LSD post hoc test (Fig. 2 *A*–*F*). Open circles represent biological replicates.

because the half-life and the steady-state concentration of albumin are decreased in FcRn-deficient individuals and animals, it was proposed that FcRn diverts not only IgG but also albumin from intracellular degradation, prolonging the life spans of both proteins (3, 11, 14, 15). Further, both the conditional deletion of FcRn in endothelial and hematopoietic cells and renal deficiency of FcRn have been shown to cause hypoalbuminemia (16–18). In the latter case, the hypoalbuminemia is associated with albuminuria, as is consistent with FcRn's recently identified role in retrieving albumin from the urinary stream to prevent its loss (17–19).

Albumin synthesis takes place in the hepatocyte. This specialized parenchymal cell is also a major cellular site for the expression of FcRn, which is distributed intracellularly and localized to the canalicular (apical) and sinusoidal (basal) membranes (20–23). However, the functional role played by FcRn in hepatocytes and its consequences for the fate of albumin are unknown. Here we show that FcRn in hepatocytes is critical for directing albumin into the vascular space and away from the bile, thereby also influencing liver susceptibility to injury by toxins capable of binding to albumin.

Results

Hepatic FcRn Deficiency Causes Hypoalbuminemia and Albumin Loss into Bile. We first examined the endogenous levels of albumin in the bloodstream and bile of WT ($Fcgrt^{+/+}$), FcRn-heterozygous ($Fcgrt^{+/-}$), and FcRn-deficient ($Fcgrt^{-/-}$) mice. Consistent with prior published results (1, 3), we observed a significant decrease in the serum levels of albumin (Fig. 1*A*) and IgG (Fig. 1*B*) in $Fcgrt^{-/-}$ mice compared with $Fcgrt^{+/+}$ and $Fcgrt^{+/-}$ mice (Table 1). In contrast, the levels of albumin (Fig. 1*A*) and IgG (Fig. 1*B*) detected in gallbladder were significantly elevated in $Fcgrt^{-/-}$ mice relative to those observed in WT and heterozygous littermate controls.

To determine whether the liver itself was responsible for the hypoalbuminemia and albumin loss into the bile observed in the total absence of FcRn, we generated $Alb^{Cre}Fcgrt^{fl/fl}$ mice by crossing $Fcgrt^{fl/fl}$ mice (16) with mice expressing the *Cre* recombinase under control of the albumin enhancer/promoter [B6.Cg-Tg(Alb-cre)21Mgn/J, hereafter called "Alb^{Cre} mice"], which deletes target genes in hepatocytes (Fig. S1*A*) and cholangiocytes (24, 25), a minor subset of cells in the liver whose expression of FcRn has not been described (23, 26). $Alb^{Cre}Fcgrt^{fl/fl}$ mice exhibited a significant decrease in serum albumin together with increased albumin loss into the bile (Fig. 1*C*) that was proportional to the levels observed in the serum and bile of $Fcgrt^{-/-}$ mice totally lacking FcRn expression (Fig. 1*A*). The observed increase in bile albumin was not caused by a nonspecific increase in the permeability of the liver, because no differences in the levels of FITC-labeled dextran, with a molecular weight equivalent to albumin, were observed in the bile of $Fcgrt^{-/-}$ mice or WT mice 24 h after i.v. injection (Fig. S1*B*). In comparison, liver-specific deletion of *Fcgrt* did not cause hypogammaglobulinemia and caused only a trend toward increased levels of IgG in the bile (Fig. 1*D*). Notably, both the parental mouse lines, Alb^{Cre} and $Fcgrt^{fl/fl}$, displayed normal circulating albumin and IgG levels (Fig. S1*C* and Table 1). In contrast, the absence of FcRn in $CD11c^{+}$ cells, as observed in $Itgax^{Cre}Fcgrt^{fl/fl}$ mice (hereafter called "$Cd11c^{Cre}Fcgrt^{fl/fl}$ mice"), did not affect circulating or bile albumin levels (Fig. 1*E*) or bile IgG levels, although it did result in hypogammaglobulinemia (Fig. 1*F*). Thus, liver cells, most likely hepatocytes, and cells of the hematopoietic system play analogous, nonredundant roles in maintaining albumin and IgG levels, respectively, in the circulation, and the absence of FcRn expression in the liver causes significant albumin loss into the bile without changes in serum IgG levels.

FcRn Regulates Albumin Recycling, Transport, and the Vectoral Accumulation of Albumin in Polarized Epithelia. We next sought to understand the mechanisms by which hepatic FcRn maintains albumin in the circulation and prevents its loss into the bile. In the absence of a well-validated polarized hepatocyte-derived cell line, we first investigated the ability of Madin–Darby canine kidney II (MDCK II) cells transfected with either human FcRn (hFcRn) and human β_2m (hβ_2m) or rat FcRn (rFcRn) and rat β_2m (rβ_2m), or with only their respective β_2m (vector) as control, to transcytose albumin. These cells polarize efficiently on transwell inserts and have been used previously to model the transcytosis of IgG (8, 9, 27, 28). Indeed, hFcRn/hβ_2m, but not vector control cells, were able to transport human (Fig. 2*A*) and rat albumin (Fig. 2*B*) in apical-to-basal (A→B) and basal-to-apical (B→A) fashion, consistent

Table 1. Serum and bile levels of albumin and IgG in *Fcgrt*-sufficient and -deficient mice

	Albumin		IgG	
Strain	Serum, mg/mL	Bile, mg/mL	Serum, mg/mL	Bile, μg/mL
WT (n = 7)	29.58 ± 3.6	0.21 ± 0.036	15.0 ± 1.00	1.27 ± 0.77
$Fcgrt^{-/-}$ (n = 8)	11.85 ± 1.46	0.58 ± 0.09	7.08 ± 1.56	3.71 ± 0.37
$FCGRT^{TG}$ (n = 9)	33.72 ± 4.65	0.35 ± 0.047	10.52 ± 2.51	3.21 ± 0.78
Alb^{Cre} (n = 4)	27.918 ± 1.599	N.p.	10.651 ± 1.205	N.p.
$Alb^{Cre}Fcgrt^{fl/fl}$ (n = 6)	18.16 ± 0.51	0.57 ± 0.1	11.52 ± 2.51	5.11 ± 1.42
WT-$Fcgrt^{fl/fl}$ (n = 6)	32.05 ± 1.63	0.14 ± 0.01	12.35 + 2.92	2.3 ± 1.54
$Cd11c^{Cre}Fcgrt^{fl/fl}$ (n = 6)	24.506 ± 1.85	0.15 ± 0.01	6.04 ± 2.88	0.33 ± 0.11
WT-$Fcgrt^{fl/fl}$ (n = 8)	24.2 ± 1.08	0.15 ± 0.01	14.68 ± 1.71	0.93 ± 0.39

N.p., not performed.

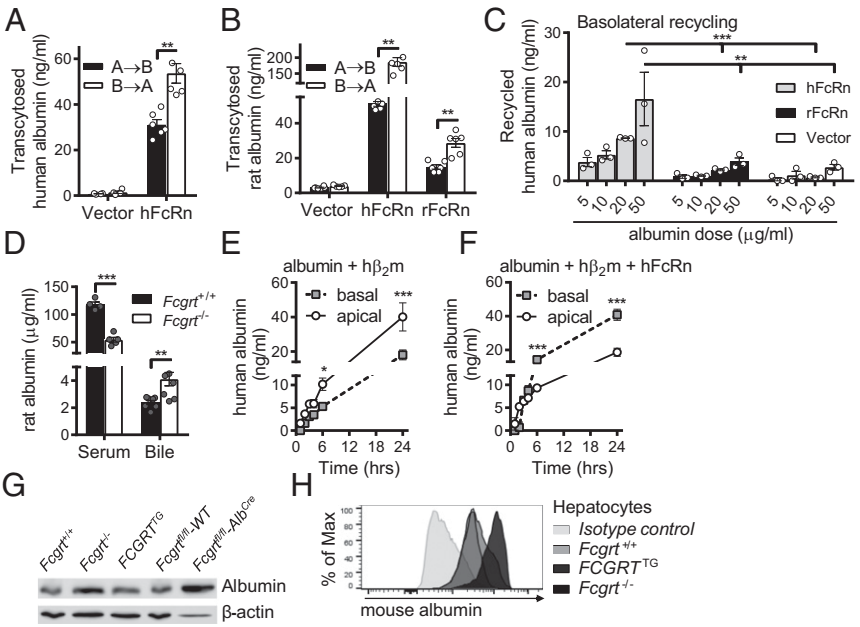

Fig. 2. Mechanisms of FcRn-mediated albumin transport. (*A*) Transcytosis of human albumin by MDCK II cells expressing hβ$_2$m only (vector) or coexpressing hFcRn and hβ$_2$m (hFcRn) (**$P < 0.01$). (*B*) Transcytosis of rat albumin by MDCK II cells expressing rβ$_2$m only (vector), coexpressing hFcRn and hβ$_2$m (hFcRn), or coexpressing rFcRn and rβ$_2$m (rFcRn) (**$P < 0.01$). (*C*) Basolateral recycling of human albumin by MDCK II cells expressing hFcRn/hβ$_2$m (hFcRn), rFcRn/rβ$_2$m (rFcRn), or rβ$_2$m only (vector) (**$P <$ 0.01, ***$P < 0.001$). (*D*) Bile and serum levels of rat albumin in WT and *Fcgrt*$^{-/-}$ mice 24 h after i.v. administration of 100 μg rat albumin ($n = 4$–6; **$P < 0.01$, ***$P <$ 0.0001). (*E* and *F*) Detection of newly biosynthesized albumin in polarized MDCK II cells coexpressing hβ$_2$m and human albumin (*E*) or hβ$_2$m, human albumin, and hFcRn (*F*) (*$P < 0.05$; ***$P < 0.01$). (*G*) Total albumin levels in liver homogenates from *Fcgrt*$^{-/-}$, *Fcgrt*$^{+/+}$, *FCGRT*^{TG}, *Fcgrt*$^{fl/fl}$-*WT*, and *Fcgrt*$^{fl/fl}$-*Alb*^{Cre} mice. Representative blots from one mouse are displayed ($n = 2$–3). (*H*) Primary mouse hepatocytes were isolated from *Fcgrt*$^{-/-}$, *Fcgrt*$^{+/+}$, and *FCGRT*^{TG} mice and were fixed, permeabilized, and stained for intracellular albumin. Representative histograms of albumin staining vs. isotype control are displayed. Open circles represent replicates. Gray-filled circles represent replicates. Gray-filled circles represent biological replicates. Data were statistically analyzed by unpaired Student *t* test (*A*–*C*, *E*, and *F*) or two-way ANOVA with Fisher's LSD post hoc test (*D*).

with a bidirectional mechanism of transcytosis and the differential ability of hFcRn to bind to different albumin orthologs (11). In that respect, heterogeneity in the binding of FcRn orthologs to albumin orthologs has been observed. In particular, hFcRn has been shown to possess higher affinity to mouse and rat albumin than to the human ortholog, as determined by surface plasmon resonance (SPR) analyses. In addition, both mFcRn and rFcRn exhibit weak binding to human albumin compared with their strong binding to the mouse and rat albumin orthologs (11). Similarly, rFcRn/rβ$_2$m-transfected MDCK II cells, but not vector control cells, exhibited bidirectional transcytosis of rat albumin (Fig. 2*B*), illustrating that human and rodent FcRn are capable of mediating the bidirectional transcytosis of albumin in a polarized epithelial cell model.

We next assessed whether polarized MDCK II cells were able to recycle albumin in the presence or absence of hFcRn/hβ$_2$m. Notably, human albumin was recycled efficiently at the basal surface of hFcRn/hβ$_2$m-expressing MDCK II cells in a dose-dependent manner but not by vector control or, as another negative control, by rFcRn/rβ$_2$m-expressing MDCK II cells (because rFcRn binds weakly to human albumin, as explained above) (Fig. 2*C*) (29, 30). Furthermore, as is consistent with defective albumin trafficking and increased leakage into the bile in the absence of FcRn in vivo, when rat albumin was injected into WT or *Fcgrt*$^{-/-}$ mice and was measured 24 h later, rat albumin levels were significantly higher in bile and lower in serum from FcRn-deficient animals than in serum from WT controls (Fig. 2*D*). Thus, exogenous rat albumin was lost more readily in the bile in the absence of FcRn.

To understand the consequences of FcRn coexpression in cells actively producing albumin, we examined the ability of FcRn to control the net accumulation of newly synthesized albumin on either side of a polarized epithelial surface. To do so, MDCK II cells expressing hβ$_2$m alone (vector control) or expressing hFcRn/hβ$_2$m were transfected with human albumin, and the rates of newly synthesized albumin accrued as apical and basal secretions were monitored over time. MDCK II cells expressing human albumin with hβ$_2$m released significantly higher concentrations of albumin in the apical chamber (modeling the canalicular surface of a hepatocyte) than in the basolateral chamber (modeling the sinusoidal surface of a hepatocyte) at all time points analyzed (Fig. 2*E*). This trend was reversed in MDCK II cells coexpressing hFcRn together with hβ$_2$m and human albumin, for which the predominant direction of albumin accretion was basolateral (Fig. 2*F*). These data suggest that FcRn may facilitate the export of albumin in the physiologic direction and that this export is further consolidated through basal recycling and potential apical scavenging of albumin.

We further examined the levels of intracellular albumin in MDCK II cells expressing albumin in the presence (hFcRn/hβ$_2$m) or absence (hβ2m alone) of FcRn by flow cytometry and observed an intracellular accumulation of albumin in the absence of hFcRn (Fig. S2*A*). Furthermore, *Fcgrt*$^{-/-}$ or *Alb*^{Cre}*Fcgrt*$^{fl/fl}$ mice, despite their hypoalbuminemic condition, were characterized by an increased intracellular hepatocyte albumin content compared with WT (*Fcgrt*$^{+/+}$ or *Fcgrt*$^{fl/fl}$) control mice, as shown by immunoblotting (Fig. 2*G* and Fig. S2*B*) and by intracellular flow cytometry (Fig. 2*H* and Fig. S2*C*) analysis of hepatocytes purified from perfused livers. Thus, as shown in MDCK cells and primary hepatocytes, newly synthesized albumin accumulates intracellularly in the absence of FcRn.

Taken together, these results suggest that in hepatocytes FcRn first exerts its protective effects on albumin by facilitating the vectorial delivery of albumin in the physiologic basolateral direction. FcRn-mediated albumin protection is further augmented by its basal recycling and, potentially, by the apical scavenging functions implied by the A→B albumin transcytosis that was observed.

Hepatic FcRn Renders the Liver Susceptible to the Effects of an Hepatocyte Toxin. In addition to preserving the colloid osmotic pressure, albumin also possesses vital antioxidant properties and is an important carrier protein that binds to and transports numerous elements, nutrients, proteins, and sometimes toxins (31). In the latter case, albumin-bound toxins might persist longer in the circulation, or albumin binding might decrease toxicity by decreasing free toxin levels. Indeed, one of the most commonly used analgesics, acetaminophen (para-acetylaminophenol, APAP), is known to bind albumin in the circulation (32) and is toxic to the liver at high doses (33, 34). When ingested in excess (above 10 g/d or 200 mg/kg for humans), the hepatocyte glucuronide pathway is saturated, resulting in the production and accumulation of a toxic byproduct, *N*-acetyl-p-benzo-quinoneimine (NAPQI) (35). NAPQI depletes glutathione (GSH) and binds in particular to mitochondrial proteins, mainly to the amino acid cysteine, causing oxidative stress, mitochondrial damage, and ultimately hepatocyte death (34, 36). We therefore hypothesized that FcRn affects the sensitivity of the liver to toxins, using APAP as a model of liver toxicity.

To examine this question, we took advantage of a previously described humanized mouse strain that expresses hFcRn under the control of human endogenous FcRn promoter as well as $h\beta_2m$ and is deficient in mouse FcRn [B6.Cg-*Fcgrt*^{tm1Dcr}Tg(FCGRT)32Dcr/DcrJ mice, hereafter referred to as "*FCGRT*^{TG} mice"] (1, 7). Immunostaining of liver sections showed that human FcRn was distributed in a vesicular pattern within hepatocytes of *FCGRT*^{TG} mice similar to that described in other polarized epithelial cell types (8), with evidence of expression on both the sinusoidal (basal) and canalicular (apical) membranes in hepatocytes, as predicted by previous studies (Fig. S3*A*) (21–23). As is consistent with the ability of hFcRn to bind to mouse albumin (29), *FCGRT*^{TG} mice displayed cell-associated (Fig. 2 *G* and *H* and Fig. S2 *B* and *C*), circulating, and bile (Fig. 3*A*) levels of albumin similar to those of *Fcgrt*$^{+/+}$ (WT) mice. Together, these studies support the utility of *FCGRT*^{TG} mice as a model of human FcRn function in the liver.

To investigate the toxicity of APAP in *Fcgrt*$^{-/-}$, *Fcgrt*$^{+/+}$, and *FCGRT*^{TG} mice, we administered a lethal dose of APAP (600 mg/kg) i.p. and found that *Fcgrt*$^{-/-}$ mice exhibited significantly greater survival than WT or *FCGRT*^{TG} mice (Fig. 3*B*). Importantly, this protection was associated with increased excretion of APAP into the bile over time as determined via bile duct cannulation (Fig. 3*C*) and with decreased levels of APAP in the serum of *Fcgrt*$^{-/-}$ mice (Fig. 3*D*) relative to WT and *FCGRT*^{TG} controls. We also found evidence for APAP in association with albumin in the bile of *Fcgrt*$^{-/-}$ mice exposed to APAP (Fig. S3 *B* and *D*). In SPR experiments, neither APAP nor NAPQI binding to albumin interfered with albumin's ability to bind to FcRn, in contrast to the long-chain fatty acid C18, oleate, which binds albumin and blocks its interaction with FcRn (Fig. S3*E*) (37). These changes in APAP levels in the bile and serum were associated with significantly lower serum alanine aminotransferase (ALT) levels in *Fcgrt*$^{-/-}$ mice than in WT or *FCGRT*^{TG} mice 8 h after sublethal APAP administration (400 mg/kg) (Fig. 3*E*).

To determine whether FcRn expression by hepatocytes contributes to the sensitivity of the liver to APAP-associated hepatotoxicity, we administered a lethal dose of APAP to *Alb*^{Cre}*Fcgrt*$^{fl/fl}$ mice and compared their survival with that of WT littermate

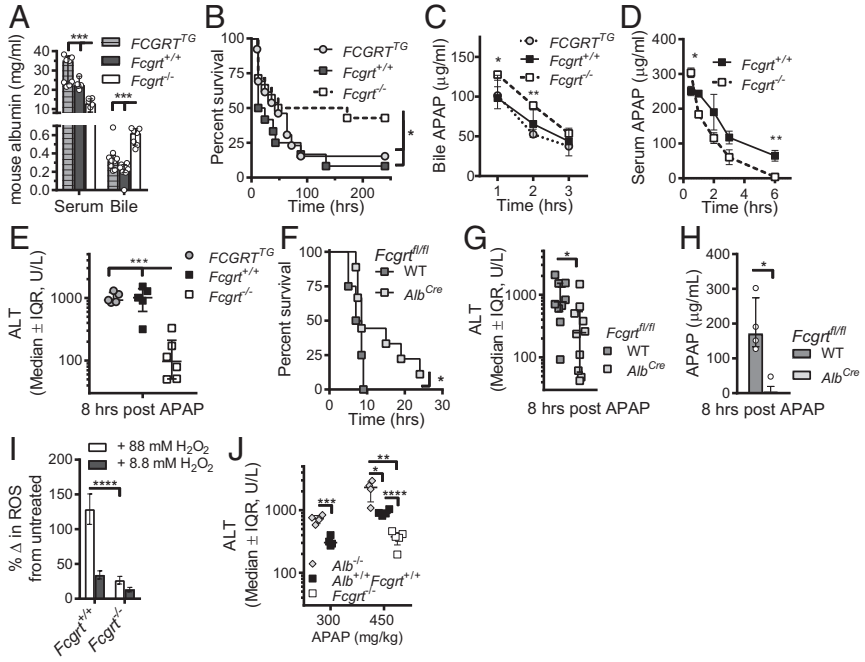

Fig. 3. Relevance of FcRn deficiency in an APAP toxicity model. (*A*) Bile and serum levels of mouse albumin in *Fcgrt*$^{-/-}$, *Fcgrt*$^{+/+}$, and *FCGRT*^{TG} mice (n = 4–7 mice per group; ***$P < 0.001$). (*B*) Survival curves after lethal APAP administration (600 mg/kg) in *Fcgrt*$^{-/-}$ (n = 14), *Fcgrt*$^{+/+}$ (n = 12), and *FCGRT*^{TG} (n = 13) (*$P = 0.0486$). (*C*) Excretion of APAP into the bile after a lethal dose of APAP in *Fcgrt*$^{+/+}$, *Fcgrt*$^{-/-}$, and *FCGRT*^{TG} mice (n = 4 per group; *$P < 0.05$, **$P < 0.01$). (*D*) Serum APAP levels in WT and *Fcgrt*$^{-/-}$ mice after a lethal dose of APAP (n = 7 per group; *$P = 0.0185$ **$P = 0.0049$). (*E*) Serum ALT levels 8 h after sublethal APAP administration (400 mg/kg) to *Fcgrt*$^{-/-}$, *Fcgrt*$^{+/+}$, and *FCGRT*^{TG} mice (n = 5–6; ***$P < 0.001$). (*F*) Survival curves after lethal APAP administration (600 mg/kg) to WT (*Fcgrt*$^{fl/fl}$-*WT*) and *Fcgrt* liver-specific–deficient (*Fcgrt*$^{fl/fl}$*Alb*^{Cre}) mice (n = 5–9; *$P < 0.05$). (*G* and *H*) Serum ALT (*G*) and APAP (*H*) levels 8 h after sublethal APAP administration (400 mg/kg) to *Fcgrt*$^{fl/fl}$-*WT* and *Fcgrt*$^{fl/fl}$-*Alb*^{Cre} mice [n = 9 or 10, pooled from three experiments (*G*) or n = 4 (*H*), *$P < 0.05$]. (*I*) Intracellular levels of ROS in *Fcgrt*$^{+/+}$ or *Fcgrt*$^{-/-}$ mouse primary hepatocytes (****$P < 0.0001$). Levels of oxidative stress were determined using a cell-permeable fluorescence probe, the chloromethyl derivative of H_2DCF-DA (CM-H_2DCF-DA), which is oxidized to fluorescent DCF. Cells were left untreated or were treated with different concentrations of H_2O_2 to increase intracellular levels of oxidative stress. The percent of change (%Δ) in ROS was calculated by subtracting the DCF mean fluorescence intensity (MFI) of untreated cells from the DCF MFI of H_2O_2-treated cells. (*J*) Serum ALT levels 8 h after administration of two different sublethal doses of APAP (300 and 450 mg/kg) in *Alb*$^{-/-}$, *Alb*$^{+/+}$*Fcgrt*$^{+/+}$, and *Fcgrt*$^{-/-}$ mice (n = 4–5; *$P = 0.019$; **$P < 0.0013$; ***$P = 0.0006$; ****$P < 0.00011$). Open circles represent biological replicates. Data were statistically analyzed by one-way ANOVA (*A* and *E*), two-way ANOVA (*I*), unpaired Student *t* test (*C*, *D*, *G*, *H*, and *J*), or Mantel–Cox test (*B* and *F*). IQR, interquartile range; U/L, units per liter.

controls (WT-$Fcgrt^{fl/fl}$). $Alb^{Cre}Fcgrt^{fl/fl}$ mice exhibited superior survival after lethal APAP administration (600 mg/kg) (Fig. 3*F*), as did $Fcgrt^{-/-}$ mice (Fig. 3*B*). Additionally, mice with liver-specific deletion of FcRn displayed significantly decreased circulating ALT (Fig. 3*G*) and serum APAP levels (Fig. 3*H*) 8 h after sublethal APAP (400 mg/kg) administration. Consequently, FcRn-deficient hepatocytes are protected from APAP-induced toxicity in association with decreased serum levels of APAP.

We hypothesized that the protection from APAP-mediated hepatotoxicity in FcRn-deficient mice is dependent on either the loss of albumin into the bile, resulting in the removal of APAP and its metabolites as described above, and/or on the accumulation of albumin in the hepatocyte, where it serves as an antioxidant through the unpaired cysteine 34 residue in humans and mice and potentially cysteine 579 in mice (38). To investigate whether FcRn influences the antioxidant buffering capacity of albumin, we measured reactive oxygen species (ROS) content using 2′,7′-dichlorodihydrofluorescein diacetate (DCFH-DA) staining in $Fcgrt^{-/-}$ and $Fcgrt^{+/+}$ hepatocytes after exposure to hydrogen peroxide (H_2O_2). As is consistent with the elevated intracellular levels of albumin observed in the absence of FcRn (Fig. 2 *G* and *H* and Fig. S2), we observed lower levels of ROS in primary $Fcgrt^{-/-}$ hepatocytes than in $Fcgrt^{+/+}$ hepatocytes (Fig. 3*I*). Therefore, the loss of FcRn in hepatocytes results in albumin retention, which correlates with greater antioxidant buffering capacity.

To confirm these results, we assessed ROS production upon H_2O_2 or APAP treatment in MDCK II cells expressing human albumin in the presence or absence of hFcRn/hβ_2m; these cells accumulate albumin in the absence of functional FcRn (Fig. S2*A*). MDCK II cells expressing hβ_2m/human albumin were more resistant to H_2O_2 and APAP treatment and generated lower amounts of ROS than cells expressing hβ_2m alone (vector), cells expressing hβ_2m/hFcRn, or cells coexpressing hβ_2m/hFcRn and human albumin (Fig. S3 *F* and *G*). This finding was reflected further in the greater survival of hβ_2m/human albumin-positive MDCK II cells upon identical H_2O_2 treatment (Fig. S3*H*).

To validate further the central role of albumin in FcRn-dependent protection from APAP toxicity, we assessed the response of albumin-deficient ($Alb^{-/-}$) mice to toxic APAP doses. These experiments revealed that $Alb^{-/-}$ mice are more susceptible to APAP administration, as illustrated by elevated serum ALT levels, than detected in WT ($Alb^{+/+}Fcgrt^{+/+}$) mice 8 h after APAP administration (Fig. 3*J*). Thus, these studies show that APAP protection depends on the transporting and antioxidant activities of albumin.

Antibody-Mediated Disruption of Human FcRn–Albumin Interactions Can Prevent APAP-Induced Hepatotoxicity. In light of these results, we next sought to determine whether specific pharmacologic blockade of albumin–FcRn interactions would protect the liver from toxic APAP exposure as observed in $Fcgrt^{-/-}$ and $Alb^{Cre}Fcgrt^{fl/fl}$ mice. Given that $FCGRT^{TG}$ mice were as susceptible as WT mice to APAP hepatotoxicity, we focused our attention on this humanized model to permit the application of human FcRn-specific agents. To do so, we used a previously described mouse anti-human FcRn monoclonal antibody, ADM31, which binds in the nanomolar range at both pH 7.4 and pH 6.0 and specifically blocks the interaction site for albumin but not for IgG (39, 40). In the in vitro studies with MDCK II cells expressing hFcRn/hβ_2m, pretreatment with ADM31, but not with an IgG2b isotype control, inhibited the transcytosis of human albumin (Fig. 4*A*). Furthermore, we observed significant hypoalbuminemia as well as albumin loss into the bile (Fig. S4*A*) 16 h after i.v. administration of ADM31 to naive $FCGRT^{TG}$ mice as compared with untreated or IgG2b isotype-treated control mice. In vitro treatment of primary hepatocytes from $FCGRT^{TG}$ mice with ADM31, but not with the isotype control, also resulted in hepatocyte accumulation of albumin (Fig. S4 *B* and *C*). As shown in Fig. 4*B*, ADM31 treatment 16 h before lethal APAP administration also significantly improved the survival of $FCGRT^{TG}$ mice to a level similar to that observed in $Fcgrt^{-/-}$ mice and significantly longer than seen for untreated $FCGRT^{TG}$ mice or $FCGRT^{TG}$ mice treated with the IgG2b isotype. In addition, pretreatment with ADM31, but not with the isotype control, resulted in significantly decreased serum ALT levels in the circulation 8 h after sublethal APAP administration (Fig. 4*C*) and decreased levels of phosphorylated JNK (p-JNK) in liver tissues at 2 h after APAP administration (Fig. S4 *D* and *E*). JNK phosphorylation actively regulates NAPQI-induced mitochondrial GSH depletion, dysfunction, and hepatocyte death (41). Histological analysis of H&E-stained liver sections confirmed a significant reduction in necrotic areas in ADM31-treated mice in this preventative model (Fig. 4 *D* and *E*). Moreover, the protection afforded by albumin–FcRn blockade with the ADM31 monoclonal antibody in the context of APAP administration was associated with decreased albumin in the circulation (Fig. S4*F*) and increased biliary albumin loss (Fig. S4*G*).

A Peptide Mimetic Can Disrupt Human FcRn–Albumin Interactions and Provide Protection Against APAP-Induced Hepatotoxicity. To substantiate our findings, we sought a different approach relying on a previously described phage-display library (42) to identify a heptadecamer (17-mer) peptide, SYN1753 (Ac-RYFCTKWKHGWCEEVGT-$CONH_2$), capable of binding to soluble hFcRn (shFcRn) and specifically inhibiting its interaction with albumin (Table 2). We confirmed the specificity of the SYN1753 for the albumin-binding site on hFcRn by solving the X-ray cocrystal structure of the complex [Protein Data Bank (PDB) ID code: 5BJT] (Fig. 4 *F*–*H* and Table S1). This complex consisted of a pair of SYN1753 peptides forming contacts with a single hFcRn molecule (Fig. 4*F*) at a location that defined specific albumin-binding epitopes. These sites were centered on several previously identified albumin contact residues in FcRn, Phe157 (F157), His161 (H161), and His166 (H166) (Fig. 4 *G* and *H*), and provide evidence for the bona-fide nature of this FcRn–albumin–binding mimic (12, 43). Furthermore, comparison of the FcRn:$(SYN1753)_2$ complex with previously published FcRn–albumin crystallographic studies (37) showed that the pair of SYN1753 peptides bind hFcRn at the same binding site as domain I of albumin (Fig. 4*I*). The N and C termini of the two SYN1753 peptides were in close proximity to each other in the X-ray crystal structure (Fig. 4*G*), suggesting that a covalently linked dimer may represent a more optimized peptide. We therefore generated the 37-aa dimeric peptide SYN3258 by fusing two SYN1753 peptides with a flexible glycine linker [Ac-(SYN1753)-GGG-(SYN1753)-$CONH_2$]. Both parental monomeric (SYN1753) and dimeric (SYN3258) peptides were able to inhibit FcRn-directed transcytosis of albumin in MDCK II cells relative to that observed with a scrambled control peptide (Fig. S4*H*). When continuously administered at a dose of 40 mg/kg body weight per day via an i.p. pump, SYN3258, but not a control peptide, not only protected the liver from injury after lethal APAP administration (Fig. 4*J*) but also improved mouse survival (Fig. S4*I*). As expected, SYN3258 treatment also led to significant hypoalbuminemia and increased albumin loss into the bile (Fig. S4*J*). These studies with a peptide mimetic confirm that disrupting albumin interactions with hFcRn protects the liver from the toxic effects of APAP.

Antibody-Mediated Protection Against APAP-Induced Hepatotoxicity Through Disruption of Human FcRn–Albumin Interactions Can Be Extended to a Therapeutic Setting. Having shown that albumin–FcRn blockade before APAP administration prevents hepatotoxicity, we examined the ability of albumin–FcRn blockade to protect the liver in a therapeutic rather than preventative model. To do so, we administered the ADM31 monoclonal antibody 2 h after lethal exposure to APAP (Fig. S5*A*). As shown in Fig. S5*B*, therapeutic administration of ADM31 after lethal APAP treatment improved, although nonsignificantly, the survival of $FCGRT^{TG}$ mice compared with untreated mice or mice treated with the IgG2b isotype.

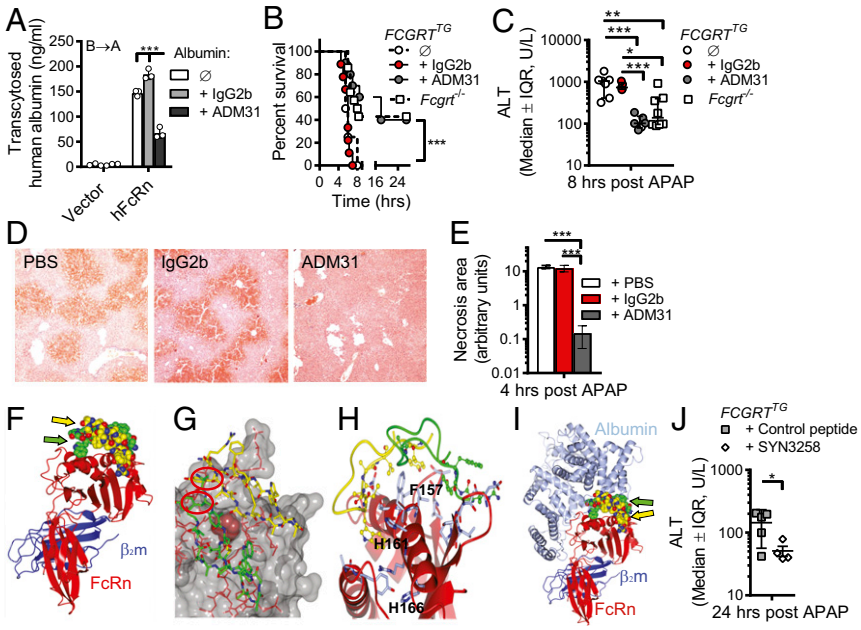

Fig. 4. Antibody- or peptide-mediated disruption of the human FcRn–albumin interactions decreases chemical hepatotoxicity. (*A*) Transcytosis of human albumin in MDCK II cells expressing hFcRn and hβ_2m (hFcRn) or hβ_2m alone (vector) in the presence of ADM31 or IgG2b (***$P < 0.001$). Open circles represent replicates. (*B* and *C*) Survival curves after lethal (600 mg/kg) APAP administration (*B*) and serum ALT levels 8 h after sublethal APAP administration (400 mg/kg) (*C*) in *Fcgrt*$^{-/-}$ mice (n = 8–14), untreated *FCGRT*^{TG} mice (n = 4–7), and *FCGRT*^{TG} mice that received either ADM31 (n = 6–10) or IgG2b isotype control (n = 5–9) (30 mg/kg) 16 h before APAP administration (***$P = 0.0002$ in *B*; *$P = 0.0391$, **$P = 0.0021$, ***$P < 0.0004$ in *C*). (*D* and *E*) Liver H&E staining (*D*) and cumulative pathology scores (*E*) from PBS-treated *FCGRT*^{TG} mice and *FCGRT*^{TG} mice that received either ADM31 or IgG2b isotype control 16 h before APAP administration, as above (n = 3; ***$P < 0.0002$). (*F*) Illustration of the solved cocrystal structure of the shFcRn:hβ_2m:$(SYN1753)^2$ complex. The FcRn heavy chain (red) with hβ_2m (blue) interacts with two SYN1753 peptides (yellow and green spheres indicated by yellow and green arrows). These figures were drawn using the PyMOL program (www.pymol.org). (*G*) Space-fill representation highlighting the pair of SYN1753 peptides bound to the FcRn surface around Phe157 (magenta) and the close proximity (red circles) of the N terminus of the first SYNT1753 peptide (yellow sticks) to the C terminus of the second SYNT1753 peptide (green sticks) that led to the generation of SYNT3258 peptide. (*H*) Both SYN1753 peptides are centered around FcRn residues F157, H161, and H166. (*I*) The area of SYN1753 peptides interaction with FcRn spans the area of FcRn-albumin (metallic blue) interaction. (*J*) Serum ALT levels 24 h after a lethal dose of APAP was administered to *FCGRT*^{TG} mice to which SYN3258 or a cyclic control peptide were continuously delivered at a dose of 40 mg/kg body weight per day via an i.p. pump (n = 6, *$P <$ 0.05). Data were analyzed statistically by one-way ANOVA (*E* and *J*), two-way ANOVA with Fisher's LSD post hoc test (*A* and *C*), or Mantel–Cox test (*B*). IQR, interquartile range; U/L, units per liter. (Magnification: 40× in *D*.)

In a separate experimental cohort with sublethal APAP administration (400 mg/kg), we further compared the effectiveness of albumin–FcRn blockade to treatment with the standard clinical antidote, *N*-acetylcysteine (NAC), which reduces APAP toxicity by replenishing liver stores of the antioxidant GSH (44), and observed that ADM31 was equally as effective as NAC in reducing circulating ALT levels in *FCGRT*^{TG} mice in contrast to mice treated with the IgG2b isotope (Fig. 5*A*). Finally, to provide further relevance to human treatment, we developed a humanized, affinity-matured version of ADM31. The resulting antibody (SYNT002-08) is a humanized, affinity-matured IgG4-κ monoclonal antibody containing a CH_3 C-terminal lysine deletion (ΔK478) and a serine-to-proline (S241P) mutation that stabilizes the hinge region in vivo (45). SYNT002-08 exhibited 10-fold improved binding to shFcRn compared with the parental ADM31, with a K_d of 4.0 nM at pH 7.4 and 0.6 nM at pH 6.0 (Fig. S5 *C* and *D* and Table S2). When administered to *FCGRT*^{TG}*Alb*$^{-/-}$ mice [B6.Cg-*Alb*^{em12Mvw} *Fcgrt*^{tm1Dcr}Tg(FCGRT)32Dcr/MvwJ (46)], it effectively increased albumin catabolism in a dose-dependent manner (Fig. S5*E*). Following the therapeutic protocol described above (Fig. S5*A*), serum ALT levels showed that SYNT002-08 at a dose of 10 mg/kg provided protection to *FCGRT*^{TG} mice equivalent to that provided by NAC administered 2 h after sublethal APAP challenge when compared with control treatment (with PBS or the IgG4 isotype) (Fig. 5*B*). Therefore, in a therapeutic setting, both ADM31 and SYNT002-08 antibodies that block the albumin–hFcRn interaction confer protection from toxic APAP exposure to the same extent as NAC.

Discussion

The importance of FcRn in sustaining high serum concentrations of circulating albumin is well established in both humans and mice (3, 14, 15). However, the cellular sites and the underlying mechanisms by which FcRn performs this critical function are poorly understood. The possibility that endothelial cells support albumin

Table 2. Sequence and affinities of FcRn-binding peptides

Peptide	Sequence	Competition for albumin binding to FcRn	K_d, pH 6.0, μM	K_d, pH 7.4, μM
SYN514	Ac-AGVMHCFWDEEFKCDQGGTGGGK-$CONH_2$	No	N/a	N/a
SYN571	Ac-AGRYFCTKWKHGWCEEVGTGGGK-$CONH_2$	Yes	0.5	13.1
SYN1753	Ac-RYFCTKWKHGWCEEVGT-$CONH_2$	Yes	0.5	N/a
SYN3258	Ac-RYFCTKWKHGWCEEVGTGGGRYFCTKWKHGWCEEVGT-$CONH_2$	Yes	0.0036	N/a

N/a, not available.

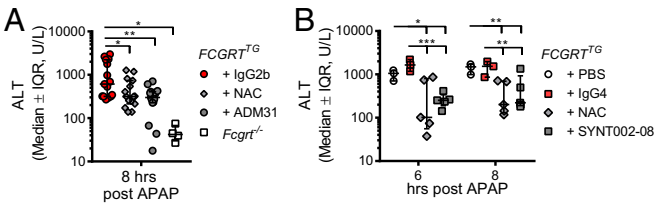

Fig. 5. Therapeutic disruption of the human FcRn–albumin interaction decreases chemical toxicity. (*A*) Serum ALT levels 8 h after sublethal APAP administration (400 mg/kg) in $Fcgrt^{-/-}$ mice or $FCGRT^{TG}$ mice that received NAC (140 mg/kg), ADM31, or IgG2b isotype control (30 mg/kg) via i.v. injection 2 h after APAP administration. (n = 4–15 from three pooled experiments; $*P < 0.05$; $**P < 0.01$). (*B*) Serum ALT levels 6 and 8 h after APAP administration (400 mg/kg) in $FCGRT^{TG}$ mice that received PBS, NAC (140 mg/kg), SYNT002-8, or IgG4 isotype control (10 mg/kg) 2 h after APAP administration (n = 3–5; $*P < 0.05$; $**P < 0.0038$; $***P < 0.001$). Data were statistically analyzed by one-way ANOVA (*A*) or two-way ANOVA with Fisher's LSD post hoc test (*B*). IQR, interquartile range; U/L, units per liter.

homeostasis through their expression of FcRn is supported by studies of Ward and colleagues using Tie2 *Cre*-mediated conditional *Fcgrt* deletion (16). Other studies have documented the involvement of renal tubular epithelial cells in albumin homeostasis (17–19). Here, we have demonstrated that parenchymal cells in the liver, mainly hepatocytes that are the source of serum albumin, require FcRn to deliver and maintain sufficient amounts of albumin in the circulation. Accordingly, the absence of FcRn in the liver results in hypoalbuminemia, the accumulation of intracellular albumin in hepatocytes, and a protein-losing biliopathy caused by loss of albumin into the bile. This effect is selective to albumin homeostasis, in that liver deficiency in FcRn does not lead to hypogammaglobulinemia or appreciable leakage of IgG into the bile. These studies uncover attributes of both hepatocytes and FcRn in ensuring the systemic functions of albumin.

In the Alb^{Cre} animal model, the cholangiocyte, another liver cell type, has also been shown to possess Cre-recombinase activity, so this cell type must be considered in the phenotype observed in $Alb^{Cre}Fcgrt^{fl/fl}$ mice (47, 48). Cholangiocytes account for ∼5% of the liver cell population, line the bile ducts, and modify bile through processes of secretion or absorption (49). Although FcRn expression in cholangiocytes has not been reported, FcRn in these cells might possess a role similar to that described in proximal tubular epithelial cells of the kidney, where it has been shown to serve in albumin reabsorption from the urine (17). If expressed, FcRn in cholangiocytes could assist in the albumin-reuptake process to minimize albumin loss into the bile. Thus, the high albumin biliary loss described in $Fcgrt^{-/-}$ or $Alb^{Cre}Fcgrt^{fl/fl}$ mice might stem from FcRn dysfunction not only in hepatocytes but conceivably also in cholangiocytes, making studies of FcRn function in cholangiocytes and its role in albumin homeostasis and susceptibility to liver toxins of great interest in future studies. Nonetheless, because we observed significant hepatocyte injury using an hepatocyte-specific toxin, as defined by histopathology and the presence of elevated circulating hepatocyte-derived enzymes after APAP administration, as well as an increase in albumin content in primary hepatocytes in $Fcgrt^{-/-}$ or $Alb^{Cre}Fcgrt^{fl/fl}$ mice, it is likely that the main cell type contributing to the observations described is the hepatocyte.

Mechanistically, our studies point to several different means by which FcRn in the hepatocyte, the site of albumin synthesis, contributes to the accumulation of albumin and its maintenance in the circulation. Similar to the endothelium (16) and proximal tubular epithelial cells of the renal collecting system (17–19), our studies suggest that FcRn in the hepatocyte basally recycles and apically scavenges albumin. This activity is supported by our results demonstrating basolateral recycling and A→B transcytosis in polarized MDCK II cells. We also observe that newly synthesized albumin accumulates apically in the absence of FcRn and accrues basally only if FcRn is expressed. These processes suggest that FcRn controls albumin homeostasis by determining the vectorial delivery of albumin to the basal surface through a combination of apical scavenging, basal recycling, and potentially facilitating albumin secretion at its site of production. Our finding of increased albumin content in the liver in the absence of FcRn thus may be a consequence of multiple factors. These include diminished vectorial delivery of albumin to the basal surface and its recycling in this location. In addition, compensatory mechanisms are engaged whereby hepatocyte biosynthesis is up-regulated, including albumin, to normalize the levels of circulating proteins, as suggested by Anderson and colleagues (20). Thus, a major function of FcRn at the site of albumin synthesis is to guide albumin into the circulation, salvage it from the canalicular compartment, and direct its delivery to the vasculature.

Significantly, we also find that these cell-intrinsic functions of FcRn render the hepatocyte susceptible to injury when exposed to certain hepatotoxins, especially those capable of albumin binding and targeting the hepatocyte. This hepatocellular sensitivity thus stems from FcRn's role in directing albumin into the circulation and away from the hepatocyte or bile and proceeds via mechanisms derived from both its carrier and antioxidant functions. In the first case, the maintenance of albumin in the circulation by hepatic FcRn may potentially prolong host exposure to a toxin when the toxin is able to bind albumin. Thus, when FcRn is genetically deleted, including conditional deletion in the liver, or when FcRn interactions with albumin are specifically blocked with monoclonal antibodies or peptidomimetics, the liver may be protected to some degree from exposure to APAP and the accompanying liver injury through the decreased albumin (and toxin) in the circulation and their increased loss in the bile.

There are some limitations to this proposed albumin–FcRn–dependent mechanism of protection that require additional experimentation in the future. For instance, it is generally acknowledged that only a limited quantity of APAP is bound to serum albumin. At normal therapeutic doses, less than 10% of APAP is bound by albumin, whereas at elevated, toxic doses the binding is 20–25% (50, 51). This low APAP carrying capacity of albumin suggests either that the flux of APAP-associated albumin is quite large or that other mechanisms are also operative. The latter possibility is likely, in view of the protection observed in therapeutic protocols wherein albumin–FcRn blockade is initiated after APAP exposure, at a time when significant APAP metabolism has already occurred (52). In accordance with human and mouse studies in which hypoalbuminemia results in an increased rate of albumin synthesis (20, 53), we detected greater intracellular albumin content in FcRn-deficient hepatocytes and upon antibody-mediated albumin–FcRn blockade. Given the antioxidant capacities of albumin, its accumulation thus can potentially provide additional buffering capacities against oxidative stress and mitochondrial injury during APAP overdose, which involves JNK-dependent, ROS-mediated injury (41). Indeed, FcRn-deficient and albumin-sufficient hepatocytes as well as albumin-expressing MDCK II cells were less susceptible to H_2O_2- or APAP-induced ROS production and the resultant death. Our studies thus suggest that the antioxidant properties of albumin are a potentially additional critical mechanism by which FcRn deficiency or blockade is protective against APAP toxicity. The relative contributions of intracellular albumin accumulation and increased ROS buffering or excretion through reversal of albumin flux into the bile and the clearance of toxic compound to the protection observed with FcRn loss or blockade remain to be elucidated in future studies. Nonetheless, both mechanisms are supported by the increased susceptibility that $Alb^{-/-}$ mice exhibit in response to APAP exposure.

Most of the current albumin-based therapies aim to imitate albumin–FcRn interactions to prolong the circulating half-life of

biologics, not to promote their degradation (40). This promotion of degradation raises the question whether inducing albumin deficiency through pharmacologic blockade would be beneficial. An accumulating body of evidence illustrates a potential detrimental effect of hypoalbuminemia on health (53, 54). At present, no individuals with FcRn-specific deficiency have been described. Mutations in the *B2M* gene resulting in the absence of β_2m expression, which affect MHC class I molecule expression in general and FcRn in particular, have been reported. These individuals, besides being immunodeficient, are characterized by reduced circulating levels of albumin (14, 15). However, given the broad effects of β_2m deficiency on immune function, extrapolations from these human subjects is impossible. Still, analbuminemic individuals, although extremely rare, have been described and are mostly asymptomatic with a normal life expectancy (55). Comparable to analbuminemic humans, albumin-deficient mice, even in the presence of hyperlipidemia, are generally healthy and breed normally (46). Similarly, FcRn-deficient mice are hypoalbuminemic, but they remain healthy throughout their life. Interestingly, a gradual increase in plasma albumin levels with age is observed in FcRn-deficient mice, consistent with a compensatory increase in the rate of hepatic albumin biosynthesis (56). In light of the absence of serious detrimental symptoms in analbuminemic hosts, given the plethora of important physiological functions carried out by albumin, it is likely that a compensatory increase in the production of other hepatic proteins and/or other physiologic changes occur in this circumstance.

As such, the evidence from human studies as well as from animal models suggests that persistent decreases or even an absence of circulating albumin is not necessarily detrimental, at least when hepatic synthetic function is intact. The results presented in this study demonstrate that short-term FcRn–albumin blockade significantly affects the biodistribution of albumin and is beneficial in an APAP model of hepatotoxicity. Whether these observations extend to other types of hepatotoxicity and whether long-term FcRn–albumin blockade would cause disadvantageous effects on the host need to be assessed in chronic models. It is of additional interest that, in certain conditions such as diabetes mellitus, post-translational modifications of albumin are associated with toxicity; in such circumstances albumin elimination may also be desirable (57–59). Thus, in particular instances, acute albumin depletion might not be harmful and, as seen here, might prove beneficial, without conferring inordinate additional risk, when albumin is carrying toxic drugs or is modified in a pathological manner.

In summary, our studies show that the hepatocyte, where albumin is synthesized, is critical to effecting FcRn-mediated control of albumin homeostasis. The mechanisms involved likely include those also used by the endothelium and renal collecting tubules (e.g., basal recycling and apical scavenging, respectively), as well as those that are unique to the hepatocyte, such as vectorial control of albumin deposition across the sinusoidal surface. Furthermore, we have shown that these albumin-trafficking properties of FcRn render the liver susceptible to injury when exposed to a hepatocyte-specific toxin that binds albumin. Thus, similar to the potential benefit of blocking IgG–FcRn interactions in the treatment of autoimmune diseases (10), protection of the liver may be achieved by therapeutic blockade of albumin–FcRn interactions.

Materials and Methods

Vectors and Cells. MDCK II cells expressing rβ_2m or hβ_2m and respective FcRn were described previously (27, 28). The human albumin gene was cloned from HepG2 cells, sequence confirmed, inserted into the pBUD4.1 vector (Invitrogen), and then transfected into MDCK II cells expressing only hβ_2m or both hβ_2m and hFcRn. Stable clones were selected by zeocin resistance and ring cloning.

Proteins and Reagents. Human albumin (Abserotec; Sigma), rat albumin (Innovative Research), human IgG (Lampire), and rat IgG (Lampire) were used for in vitro transport and in vivo experiments. APAP, NAC, DCFH-DA, and H_2O_2 were purchased from Sigma. ADM31 is an IgG2b mouse anti-human FcRn monoclonal antibody (39, 40). IgG2b isotype control was purchased from BioXCell. The mouse, human, or rat albumin and IgG levels were measured using ELISA method. Mouse (E90-134), human (E80-129), and rat (E110-125) albumin and mouse (E90-131) and human (E80-104) IgG ELISA detection kits were obtained from Bethyl Laboratories. Acetaminophen levels were determined using the Acetaminophen LiquiColor Test (Stanbio). ALT levels were measured using the ALT/SGPT Liqui-UV test (Stanbio). HBSS (Sigma) was adjusted to pH 6 or pH 7.4 using HCl or NaOH. FITC-Dextran-70 (Sigma) was diluted in PBS. The peptide inhibitors SYN1753 and SYN3258 (Biogen Idec) were diluted in PBS. The scrambled peptide used in transcytosis experiments was a 15-aa molecule generated by random rearrangement of SYN1753 sequence. The control peptide used in in vivo experiments contained the dimeric structure of SYN3258 in which three amino acids in each monomer were mutated in the following way: W7A, W11A, and V15A. Anti-human albumin-HRP and anti-mouse albumin-HRP were purchased from Bethyl Laboratories; anti-JNK, anti–p-JNK, anti-GAPDH, anti–β-actin, anti–goat-HRP, anti–mouse-HRP, and anti–sheep-HRP were purchased from Cell Signaling. Rat anti-mouse FcRn antibody was produced and validated in house. Anti-mouse albumin-FITC was purchased from Cedarlane (mCLFAG3140); anti–human-albumin-FITC (IC1455G) was purchased from R&D Systems. Mouse IgG1 and IgG2-FITC isotype controls were purchased from eBioscience.

Animals. All animal experiments were approved by the Institutional Animal Care and Use Committee of Harvard Medical School. Mice were housed in approved specific pathogen-free facilities. WT BALB/cJ (bred in house) and C57BL/6 mice (purchased from Jackson Laboratories) were used. *Fcgrt*$^{-/-}$, *Fcgrt*$^{fl/fl}$, *Alb*^{Cre}, *Cd11c*^{Cre}, *FCGRT*^{TG}, *Alb*$^{-/-}$, and *FCGRT*^{TG}*Alb*$^{-/-}$ mice were all described previously (1, 7, 16, 46, 60, 61). *Fcgrt*$^{fl/fl}$ mice were kindly provided by Dr. E. Sally Ward (Texas A&M University, College Station, TX). Hemizygous *Alb*$^{Cre+/-}$*Fcgrt*$^{fl/fl}$ (abbreviated as "*Alb*^{Cre}*Fcgrt*$^{fl/fl}$") and littermate *Alb*$^{Cre-/-}$*Fcgrt*$^{fl/fl}$ (abbreviated *as* "*WT-Fcgrt*$^{fl/fl}$") mice were used in all corresponding experiments. Hemizygous *Cd11c*$^{Cre+/-}$*Fcgrt*$^{fl/fl}$ (abbreviated as "*Cd11c*^{Cre} *Fcgrt*$^{fl/fl}$") and littermate *Cd11c*$^{Cre-/-}$*Fcgrt*$^{fl/fl}$ (abbreviated as "*WT-Fcgrt*$^{fl/fl}$") mice were used in all corresponding experiments. Nonlittermate *Fcgrt*$^{-/-}$ and *FCGRT*^{TG} mice on the BALB/cJ background were used in all experiments involving hepatotoxicity. *Alb*^{Cre}*Fcgrt*$^{fl/fl}$, *Cd11c*^{Cre}*Fcgrt*$^{fl/fl}$, *Alb*$^{-/-}$, *FCGRT*^{TG} *Alb*$^{-/-}$, and *Cd11c*$^{Cre+}$*Fcgrt*$^{fl/fl}$ mice were on the C57BL/6 background. Mice of both sexes were used for measurements of serum and bile IgG and albumin. Females were used for all APAP toxicity studies, although mice of both sexes were initially tested and showed equivalent responses.

Transcytosis, Recycling, and Secretion Assays. Albumin transcytosis assays were performed as previously described for IgG (28). Briefly, MDCK II cells expressing hβ_2m and hFcRn were grown to confluence on Transwells (Costar) and allowed to polarize over 4 d. Eighteen hours before the transcytosis experiment, the medium was changed to serum-free medium without antibiotics. On the day of the experiment, the Transwells were washed with HBSS (pH 7.4) for 20 min before being placed on a new 12-well plate (Costar). The input chamber contained HBSS (pH 6.0), and the exit chamber contained HBSS (pH 7.4); then pH-adjusted albumin was added to the input chamber. For blocking albumin transcytosis with the peptide inhibitors SYN1753 and SYN3258 or antibodies ADM31 and IgG2b, Transwells were preincubated for 20 min in HBSS (pH 6.0) before the addition of albumin in the continued presence of the peptides or antibodies. After incubation for 2 h at 36 °C and 5% (vol/vol) CO_2, the medium in the opposite chamber was harvested, and the albumin concentration was quantified using ELISA. For the recycling assay, the Transwells were washed with HBSS (pH 7.4) for 5 min before being placed on a new 12-well plate with HBSS (pH 6.0) at both chambers. After equilibration at 37 °C and 5% CO_2, pH-adjusted human albumin was added and allowed to incubate for 1 h. The Transwells then were washed with HBSS (pH 6.0) before being placed in a new 12-well plate with HBSS (pH 7.4) in both chambers. After 1-h incubation, medium was removed from the input chamber, and the albumin concentration was measured by an ELISA method. For the human albumin secretion assay the medium was changed to serum- and antibiotic-free medium on the day of the experiment. Fifty microliters of the medium from both chambers was removed periodically over 24 h, and the human albumin concentration was measured using ELISA with adjustment for volume reduction.

Preparation of Mouse Primary Hepatocytes. Primary mouse hepatocytes were isolated as described (62). Briefly, mice were anesthetized with an i.p. injection of ketamine (100 mg/kg; Webster Veterinary) plus xylazine (10 mg/kg; Webster Veterinary). The inferior vena cava was exposed, cannulated, and perfused for 5 min with liver-perfusion medium (Invitrogen), followed by a 10-min perfusion with liver-digestion medium (Invitrogen), each having been prewarmed

to 37 °C. The digested liver was diced in cold hepatocyte wash medium (Invitrogen), passed through a 100-μm strainer (Thermo Fisher Scientific), and washed three times. Cells were pelleted and resuspended in cold Williams E medium containing 10% FBS, 10^{-7} M dexamethasone, 10 μg/mL insulin, and 5 μg/mL transferrin. Viability was estimated by the Trypan Blue exclusion method. Cells were plated overnight in six-well plates (BD Biosciences) at a density of 5×10^5 cells per well.

Intracellular Albumin and FcRn Staining. Primary hepatocytes or MDCK II cells were prepared as described above, stained with Fixable Viability Dye eFluor780 (eBioscience; 65-0865-18), and were fixed and permeabilized according to instructions provided with the BD Cytofix/Cytoperm Kit (BD Biosciences; 554714). Mouse albumin-FITC or anti–human-albumin-FITC antibodies were used per the manufacturer's instructions. In-house–biotinylated ADM31 antibody was used for human FcRn staining followed by Streptavidin-PE (BioLegend; 405204). The cells were acquired on MACSQuant (Miltenyi Biotec) or CytoFLEX flow cytometer (Beckman Coulter) and were analyzed using FlowJo software (TreeStar).

Measurement of Oxidative Stress. Oxidative stress was measured using an ROS assay with DCFH-DA, which is based on the ROS-dependent oxidation of DCFH-DA to fluorescent dichlorofluorescin (DCF). MDCK II cells were trypsinized and resuspended at 1×10^6 cells/mL in HBSS. Primary hepatocytes were obtained as previously described and were resuspended at 1×10^6 cells/mL in HBSS. The cells were then plated in round-bottomed 96-well plates at 1×10^5 cells per well. After H_2O_2 or APAP treatment, cells were loaded for 15 min at 37 °C in HBSS containing 2.5 μM DCFH-DA. After cells were washed twice in cold HBSS, DCF fluorescence was measured by a flow cytometer (MACSQuant; Miltenyi), and the raw data were analyzed using the FlowJo analysis program (TreeStar). Treatments for 15 min at 37 °C with increasing concentrations of H_2O_2 were carried out to trigger ROS formation in MDCK II cells or primary hepatocytes. To measure APAP-induced ROS formation in MDCK II cells, the cells were treated with increasing concentrations of APAP for 12 h at 37 °C, 5% CO_2. To measure cell death, MDCK II cells were also stained with 7-aminoactinomycin D (7-AAD) (BD Bioscience) or DAPI dye. Results were reported as the percentage of difference from baseline DCF^+ cells and H_2O_2- or APAP-treated MDCK II cells. Cells were acquired, and data were analyzed as described above.

Bile Collection. To remove the bile from the gallbladder, mice were fasted for 4 h before being killed, and immediate laparotomy was performed to expose the gallbladder. A 30-gauge needle was inserted into the gallbladder to aspirate the bile. To remove bile by bile duct cannulation, mice were anesthetized throughout the laparotomy. An abdominal midline incision allowed the gallbladder and biliary tree to be exposed. The cystic duct was ligated with a suture. A small incision was made at the common bile duct before insertion of a PE-10 catheter (Terumo). Bile then was collected at 20-min intervals.

In Vivo Acetaminophen Experiments. For lethal acetaminophen administration, APAP was diluted in warm PBS at a concentration of 33.3 mg/mL. An acetaminophen dose of 600–700 mg/kg body weight administered i.p. was found to be lethal, as titrated in dose-findings experiments, and a dose of 600 mg/kg was used thereafter in all lethal experiments. For sublethal APAP injections, APAP was diluted in warm PBS to a concentration of 25 mg/mL, and a dose of 300–450 mg/kg was administered i.p. to mice. Animals were killed 2, 4, or 8 h after APAP administration; blood was collected via cardiac puncture, and bile was collected as described above. Livers subsequently were collected directly, formalin-fixed, paraffin-embedded, sectioned, and stained with H&E as previously described (63) or were perfused with cold PBS via the inferior vena cava and snap-frozen in liquid nitrogen for later protein analysis by Western blotting as previously described (64). All mice were fasted 4 h before being killed. For preventive antibody treatment, ADM31 or IgG2b isotype control (30 mg/kg) was administered via the tail vein 16 h before APAP administration. For therapeutic antibody treatment, ADM31 or IgG2b (30 mg/kg) and SYNT002-08 or IgG4 (10 mg/kg) were administered via the tail vein 2 h after APAP treatment. To block the interaction between FcRn and albumin, a cyclic control peptide for SYN3258 was designed in which three key residues per monomer that has been identified by alanine screening to be critical for binding between FcRn and albumin were mutated to alanines (W7A, W11A, V15A). SYN3258 or the control peptide then was administered continuously via an i.p. osmotic pump (ALZET) over a 72-h period. Before the surgical implantation of the pump, mice were anesthetized with Buprenex (0.1 mg/kg body weight) s.c. and ketamine HCl (100 mg/kg)/xylazine (10 mg/kg) i.p. Hair on the incision site was clipped, and the implantation area was disinfected by 5% iodine in 70% isopropanol. Antibiotics (100 μg/mL gentamycin) were sprayed on the area of incision to prevent infection, and skin was sutured using polypropylene suture. The total duration of the surgical procedure was around 5 min per mouse. Eighteen to twenty hours after pump implantation, a lethal dose of acetaminophen was administered i.p.

Phage Display. Peptide phage libraries, obtained from Dyax Corp., were selected for binding to biotinylated shFcRn, using three rounds of sequential pH 6 binding and pH 7.5 elution/amplification protocols. In each round, phages were incubated with biotinylated shFcRn for 30 min at room temperature in pH 6 binding buffer (50 mM MES, 150 mM NaCl, 0.1% Tween 20). After phage binding, streptavidin-coated magnetic microparticles (MG-SA; Seradyn) were added to bind the biotinylated shFcRn, and the microparticles were magnetically immobilized and washed with pH 6 binding buffer. Phage were eluted from FcRn/microparticles in pH 7.5 elution buffer (50 mM phosphate, 150 mM NaCl, 0.1% Tween 20) and were amplified between each round by infecting XL1 blue MRF′ cells and collecting cells showing phage-encoded tetracycline resistance. In the first round, 100 pfu for each unique phage peptide in each of the TN-IV, TN-10-X, TN11-I, and TN12-1 libraries were pooled and added to the selection ($1.4–3.0 \times 10^{11}$ pfu per library); for rounds 2 and 3, phage input was reduced to 10^{11} pfu total per round. FcRn-binding phage was confirmed by phage ELISA as described previously (42) and was amplified by PCR using primers 3PCRUP (5′-CGGCGCAACTATCGGTATCAAGCTG-3′) and 3PCRDN (5′-CATGTACCGTA-ACACTGAGTTTCGTC-3′), the Core PCR System II (Promega), and a cycle consisting of 94 °C for 5 min, 30× (94 °C for 15 s, 55 °C for 30 s, 72 °C for 1 min), and 72 °C for 7 min. Amplified PCR product was purified using the QIAquick PCR Prep Kit (Qiagen) and sequenced by the Tufts University Core Facility.

Phage display identified a series of peptides, including SYN514 (Ac-AGVMHCFWDEEFKCDQGGTGGGK-$CONH_2$), which was shown by competition experiments not to block FcRn–albumin interactions (Table 2). Peptide SYN514 was used during a second peptide phage screen before the addition of the phage to identify additional albumin-competitive sequences. This strategy uncovered the albumin-competitive peptide SYN571 and, through structure–activity relationships, the shorter sequence SYN1753 (Ac-RYFCTKWKHGWCEEVGT-$CONH_2$), which bound to shFcRn.

Statistical Analysis. Statistical analyses were performed using Prism (version 7.01; GraphPad Software, Inc.). Statistical significance (*P* values) was obtained using an unpaired *t* test (for comparisons between two groups), an ordinary one-way ANOVA (for comparisons between three or more groups), two-way ANOVA with Fisher's Least Significant Difference (LSD) post hoc test (for comparisons between three or more groups with two or more parameters tested), or a Mantel–Cox test (for comparisons of survival distributions). A two-sided *P* value less than 0.05 was considered significant.

ACKNOWLEDGMENTS. We thank John Badger of Zenobia Therapeutics for determining the structure of the FcRn–peptide complex; the following individuals for technical assistance and scientific advice: Erik de Muink, Victoria G. Aveson, Jie Zhang, Monica Leonard, Leona Doyle, Jennifer Danielson, Victoria Thiele, Garrett D. Hauck, Thomas Hanley, Arianna Degruttola, and Anh P. Do; and Mario Sabin for excellent care and handling of the animals. This project was supported by National Institutes of Health Grants DK071798 (to T.T.K.), DK084424 and DK048106 (to W.I.L.), DK06715 and DK48522 (to N.K.), and DK053056, DK0444319, DK088199, and DK051362 (to R.S.B.); the American Liver Foundation (T.T.K.); Canadian Institutes of Health Research (M.P.); Research Council of Norway Grants 230526/F20 and 179573/V40 (to J.T.A.); Research Council of Norway Centers of Excellence Grant 179573 (to J.T.A. and I.S.); the Alliance for Lupus Research (D.C.R. and G.C.); and Harvard Digestive Disease Center Grant DK034854 (to T.T.K., W.I.L., and R.S.B.).

1. Roopenian DC, et al. (2003) The MHC class I-like IgG receptor controls perinatal IgG transport, IgG homeostasis, and fate of IgG-Fc-coupled drugs. *J Immunol* 170(7):3528–3533.
2. Ober RJ, Martinez C, Lai X, Zhou J, Ward ES (2004) Exocytosis of IgG as mediated by the receptor, FcRn: An analysis at the single-molecule level. *Proc Natl Acad Sci USA* 101(30):11076–11081.
3. Chaudhury C, et al. (2003) The major histocompatibility complex-related Fc receptor for IgG (FcRn) binds albumin and prolongs its lifespan. *J Exp Med* 197(3):315–322.
4. Raghavan M, Bonagura VR, Morrison SL, Bjorkman PJ (1995) Analysis of the pH dependence of the neonatal Fc receptor/immunoglobulin G interaction using antibody and receptor variants. *Biochemistry* 34(45):14649–14657.
5. Ward ES, Zhou J, Ghetie V, Ober RJ (2003) Evidence to support the cellular mechanism involved in serum IgG homeostasis in humans. *Int Immunol* 15(2):187–195.
6. Yoshida M, et al. (2006) Neonatal Fc receptor for IgG regulates mucosal immune responses to luminal bacteria. *J Clin Invest* 116(8):2142–2151.

7. Yoshida M, et al. (2004) Human neonatal Fc receptor mediates transport of IgG into luminal secretions for delivery of antigens to mucosal dendritic cells. *Immunity* 20(6):769–783.
8. Dickinson BL, et al. (1999) Bidirectional FcRn-dependent IgG transport in a polarized human intestinal epithelial cell line. *J Clin Invest* 104(7):903–911.
9. Claypool SM, et al. (2004) Bidirectional transepithelial IgG transport by a strongly polarized basolateral membrane Fcgamma-receptor. *Mol Biol Cell* 15(4):1746–1759.
10. Nixon AE, et al. (2015) Fully human monoclonal antibody inhibitors of the neonatal fc receptor reduce circulating IgG in non-human primates. *Front Immunol* 6:176.
11. Chaudhury C, Brooks CL, Carter DC, Robinson JM, Anderson CL (2006) Albumin binding to FcRn: Distinct from the FcRn-IgG interaction. *Biochemistry* 45(15): 4983–4990.
12. Andersen JT, et al. (2012) Structure-based mutagenesis reveals the albumin-binding site of the neonatal Fc receptor. *Nat Commun* 3:610.
13. Pyzik M, Rath T, Lencer WI, Baker K, Blumberg RS (2015) FcRn: The architect behind the immune and nonimmune functions of IgG and albumin. *J Immunol* 194(10): 4595–4603.
14. Wani MA, et al. (2006) Familial hypercatabolic hypoproteinemia caused by deficiency of the neonatal Fc receptor, FcRn, due to a mutant beta2-microglobulin gene. *Proc Natl Acad Sci USA* 103(13):5084–5089.
15. Ardeniz Ö, et al. (2015) β2-Microglobulin deficiency causes a complex immunodeficiency of the innate and adaptive immune system. *J Allergy Clin Immunol* 136(2): 392–401.
16. Montoyo HP, et al. (2009) Conditional deletion of the MHC class I-related receptor FcRn reveals the sites of IgG homeostasis in mice. *Proc Natl Acad Sci USA* 106(8): 2788–2793.
17. Sarav M, et al. (2009) Renal FcRn reclaims albumin but facilitates elimination of IgG. *J Am Soc Nephrol* 20(9):1941–1952.
18. Tenten V, et al. (2013) Albumin is recycled from the primary urine by tubular transcytosis. *J Am Soc Nephrol* 24(12):1966–1980.
19. Sandoval RM, et al. (2012) Multiple factors influence glomerular albumin permeability in rats. *J Am Soc Nephrol* 23(3):447–457.
20. Kim J, et al. (2006) Albumin turnover: FcRn-mediated recycling saves as much albumin from degradation as the liver produces. *Am J Physiol Gastrointest Liver Physiol* 290(2): G352–G360.
21. Akilesh S, Christianson GJ, Roopenian DC, Shaw AS (2007) Neonatal FcR expression in bone marrow-derived cells functions to protect serum IgG from catabolism. *J Immunol* 179(7):4580–4588.
22. Blumberg RS, et al. (1995) A major histocompatibility complex class I-related Fc receptor for IgG on rat hepatocytes. *J Clin Invest* 95(5):2397–2402.
23. Borvak J, et al. (1998) Functional expression of the MHC class I-related receptor, FcRn, in endothelial cells of mice. *Int Immunol* 10(9):1289–1298.
24. Geisler F, et al. (2008) Liver-specific inactivation of Notch2, but not Notch1, compromises intrahepatic bile duct development in mice. *Hepatology* 48(2):607–616.
25. Sparks EE, Huppert KA, Brown MA, Washington MK, Huppert SS (2010) Notch signaling regulates formation of the three-dimensional architecture of intrahepatic bile ducts in mice. *Hepatology* 51(4):1391–1400.
26. Sampaziotis F, et al. (2015) Cholangiocytes derived from human induced pluripotent stem cells for disease modeling and drug validation. *Nat Biotechnol* 33(8):845–852.
27. Claypool SM, Dickinson BL, Yoshida M, Lencer WI, Blumberg RS (2002) Functional reconstitution of human FcRn in Madin-Darby canine kidney cells requires co-expressed human beta 2-microglobulin. *J Biol Chem* 277(31):28038–28050.
28. Kuo TT, et al. (2009) N-glycan moieties in neonatal Fc receptor determine steady-state membrane distribution and directional transport of IgG. *J Biol Chem* 284(13): 8292–8300.
29. Andersen JT, Daba MB, Berntzen G, Michaelsen TE, Sandlie I (2010) Cross-species binding analyses of mouse and human neonatal Fc receptor show dramatic differences in immunoglobulin G and albumin binding. *J Biol Chem* 285(7):4826–4836.
30. Andersen JT, et al. (2013) Single-chain variable fragment albumin fusions bind the neonatal Fc receptor (FcRn) in a species-dependent manner: Implications for in vivo half-life evaluation of albumin fusion therapeutics. *J Biol Chem* 288(33):24277–24285.
31. Varshney A, et al. (2010) Ligand binding strategies of human serum albumin: How can the cargo be utilized? *Chirality* 22(1):77–87.
32. Dearden JC, Tomlinson E (1970) Physico-chemical studies of analgesics. The protein-binding of some p-substituted acetanilides. *J Pharm Pharmacol* 22(Suppl):53S.
33. McGill MR, et al. (2013) Plasma and liver acetaminophen-protein adduct levels in mice after acetaminophen treatment: Dose-response, mechanisms, and clinical implications. *Toxicol Appl Pharmacol* 269(3):240–249.
34. Yuan L, Kaplowitz N (2013) Mechanisms of drug-induced liver injury. *Clin Liver Dis* 17(4):507–518, vii.
35. Dahlin DC, Miwa GT, Lu AY, Nelson SD (1984) N-acetyl-p-benzoquinone imine: A cytochrome P-450-mediated oxidation product of acetaminophen. *Proc Natl Acad Sci USA* 81(5):1327–1331.
36. Liu ZX, Kaplowitz N (2006) Role of innate immunity in acetaminophen-induced hepatotoxicity. *Expert Opin Drug Metab Toxicol* 2(4):493–503.
37. Schmidt MM, et al. (2013) Crystal structure of an HSA/FcRn complex reveals recycling by competitive mimicry of HSA ligands at a pH-dependent hydrophobic interface. *Structure* 21(11):1966–1978.
38. Taverna M, Marie AL, Mira JP, Guidet B (2013) Specific antioxidant properties of human serum albumin. *Ann Intensive Care* 3(1):4.
39. Christianson GJ, et al. (2012) Monoclonal antibodies directed against human FcRn and their applications. *MAbs* 4(2):208–216.
40. Sand KM, et al. (2014) Dissection of the neonatal Fc receptor (FcRn)-albumin interface using mutagenesis and anti-FcRn albumin-blocking antibodies. *J Biol Chem* 289(24): 17228–17239.
41. Gunawan BK, et al. (2006) c-Jun N-terminal kinase plays a major role in murine acetaminophen hepatotoxicity. *Gastroenterology* 131(1):165–178.
42. Mezo AR, et al. (2008) Reduction of IgG in nonhuman primates by a peptide antagonist of the neonatal Fc receptor FcRn. *Proc Natl Acad Sci USA* 105(7):2337–2342.
43. Andersen JT, Dee Qian J, Sandlie I (2006) The conserved histidine 166 residue of the human neonatal Fc receptor heavy chain is critical for the pH-dependent binding to albumin. *Eur J Immunol* 36(11):3044–3051.
44. Lauterburg BH, Corcoran GB, Mitchell JR (1983) Mechanism of action of N-acetylcysteine in the protection against the hepatotoxicity of acetaminophen in rats in vivo. *J Clin Invest* 71(4):980–991.
45. Angal S, et al. (1993) A single amino acid substitution abolishes the heterogeneity of chimeric mouse/human (IgG4) antibody. *Mol Immunol* 30(1):105–108.
46. Roopenian DC, et al. (2015) Albumin-deficient mouse models for studying metabolism of human albumin and pharmacokinetics of albumin-based drugs. *MAbs* 7(2): 344–351.
47. Xu X, et al. (2006) Induction of intrahepatic cholangiocellular carcinoma by liver-specific disruption of Smad4 and Pten in mice. *J Clin Invest* 116(7):1843–1852.
48. Dutton JR, et al. (2007) Beta cells occur naturally in extrahepatic bile ducts of mice. *J Cell Sci* 120(Pt 2):239–245.
49. Tabibian JH, Masyuk AI, Masyuk TV, O'Hara SP, LaRusso NF (2013) Physiology of cholangiocytes. *Compr Physiol* 3(1):541–565.
50. Bailey DN, Briggs JR (2004) The binding of selected therapeutic drugs to human serum alpha-1 acid glycoprotein and to human serum albumin in vitro. *Ther Drug Monit* 26(1):40–43.
51. Milligan TP, Morris HC, Hammond PM, Price CP (1994) Studies on paracetamol binding to serum proteins. *Ann Clin Biochem* 31(Pt 5):492–496.
52. Hinson JA, Roberts DW, James LP (2010) Mechanisms of acetaminophen-induced liver necrosis. *Handb Exp Pharmacol* (196):369–405.
53. Levitt DG, Levitt MD (2016) Human serum albumin homeostasis: A new look at the roles of synthesis, catabolism, renal and gastrointestinal excretion, and the clinical value of serum albumin measurements. *Int J Gen Med* 9:229–255.
54. Fanali G, et al. (2012) Human serum albumin: From bench to bedside. *Mol Aspects Med* 33(3):209–290.
55. Watkins S, Madison J, Galliano M, Minchiotti L, Putnam FW (1994) Analbuminemia: Three cases resulting from different point mutations in the albumin gene. *Proc Natl Acad Sci USA* 91(20):9417–9421.
56. Koltun M, Nikolovski J, Strong K, Nikolic-Paterson D, Comper WD (2005) Mechanism of hypoalbuminemia in rodents. *Am J Physiol Heart Circ Physiol* 288(4):H1604–H1610.
57. Dozio E, Di Gaetano N, Findeisen P, Corsi Romanelli MM (2017) Glycated albumin: From biochemistry and laboratory medicine to clinical practice. *Endocrine* 55(3): 682–690.
58. LeVine SM (2016) Albumin and multiple sclerosis. *BMC Neurol* 16:47.
59. Cohen MP (2003) Intervention strategies to prevent pathogenetic effects of glycated albumin. *Arch Biochem Biophys* 419(1):25–30.
60. Postic C, et al. (1999) Dual roles for glucokinase in glucose homeostasis as determined by liver and pancreatic beta cell-specific gene knock-outs using Cre recombinase. *J Biol Chem* 274(1):305–315.
61. Caton ML, Smith-Raska MR, Reizis B (2007) Notch-RBP-J signaling controls the homeostasis of CD8-dendritic cells in the spleen. *J Exp Med* 204(7):1653–1664.
62. Zeissig S, et al. (2012) Hepatitis B virus-induced lipid alterations contribute to natural killer T cell-dependent protective immunity. *Nat Med* 18(7):1060–1068.
63. Kaser A, et al. (2008) XBP1 links ER stress to intestinal inflammation and confers genetic risk for human inflammatory bowel disease. *Cell* 134(5):743–756.
64. Win S, Than TA, Min RW, Aghajan M, Kaplowitz N (2016) c-Jun N-terminal kinase mediates mouse liver injury through a novel Sab (SH3BP5)-dependent pathway leading to inactivation of intramitochondrial Src. *Hepatology* 63(6):1987–2003.
65. Muldrew KL, et al. (2002) Determination of acetaminophen-protein adducts in mouse liver and serum and human serum after hepatotoxic doses of acetaminophen using high-performance liquid chromatography with electrochemical detection. *Drug Metab Dispos* 30(4):446–451.
66. Mezo AR, Sridhar V, Badger J, Sakorafas P, Nienaber V (2010) X-ray crystal structures of monomeric and dimeric peptide inhibitors in complex with the human neonatal Fc receptor, FcRn. *J Biol Chem* 285(36):27694–27701.
67. Otwinowski Z, Minor W (1997) Processing of X-ray diffraction data collected in oscillation mode. *Methods Enzymol* 276:307–326.
68. McCoy AJ, et al. (2007) Phaser crystallographic software. *J Appl Crystallogr* 40(Pt 4): 658–674.
69. Jones TD, Crompton LJ, Carr FJ, Baker MP (2009) Deimmunization of monoclonal antibodies. *Methods Mol Biol* 525:405–423.
70. Schier R, et al. (1996) Isolation of high-affinity monomeric human anti-c-erbB-2 single chain Fv using affinity-driven selection. *JMol Biol* 255(1):28–43.
71. Andersen JT, et al. (2008) Ligand binding and antigenic properties of a human neonatal Fc receptor with mutation of two unpaired cysteine residues. *FEBS J* 275(16): 4097–4110.